

Received February 26, 2021, accepted March 19, 2021, date of publication March 29, 2021, date of current version April 7, 2021.

Digital Object Identifier 10.1109/ACCESS.2021.3069336

Dynamic Underwater Acoustic Channel Tracking for Correlated Rapidly Time-Varying Channels

QIHANG HUANG¹, WEI LI^{1,2}, (Member, IEEE), WEICHENG ZHAN¹,
YUHANG WANG¹, AND RONGRONG GUO¹

¹Harbin Institute of Technology, Shenzhen 518055, China

²Peng Cheng Laboratory, Shenzhen 518055, China

Corresponding author: Wei Li (li.wei@hit.edu.cn)

This work was supported in part by the National Natural Science Foundation of China under Grant 61871151, in part by the National Natural Science Foundation of Guangdong Province under Grant 2018A030313177, in part by the Guangdong Science and Technology Planning Project under Grant 2018B030322004, and in part by the Project The Verification Platform of Multi-tier Coverage Communication Network for Oceans under Grant LZC0020.

ABSTRACT In this work, we focus on the model-mismatch problem for model-based subspace channel tracking in the correlated underwater acoustic channel. A model based on the underwater acoustic channel's correlation can be used as the state-space model in the Kalman filter to improve the underwater acoustic channel tracking compared that without a model. Even though the data support the assumption that the model is slow-varying and uncorrelated to some degree, to improve the tracking performance further, we cannot ignore the model-mismatch problem because most channel models encounter this problem in the underwater acoustic channel. Therefore, in this work, we provide a dynamic time-variant state-space model for underwater acoustic channel tracking. This model is tolerant to the slight correlation after decorrelation. Moreover, a forward-backward Kalman filter is combined to further improve the tracking performance. The performance of our proposed algorithm is demonstrated with the same at-sea data as that used for conventional channel tracking. Compared with the conventional algorithms, the proposed algorithm shows significant improvement, especially in rough sea conditions in which the channels are fast-varying.

INDEX TERMS Correlated channels, model mismatch, underwater acoustic channels, channel tracking, forward-backward Kalman filter.

I. INTRODUCTION

Underwater acoustic channels are some of the most challenging channels in wireless communications [1] because they may suffer from substantial multipath interference, significant Doppler spread, and rapid time variation. Acquiring the acoustic channel state information is usually crucial for underwater acoustic communications and signal processing [2].

With the development of underwater acoustic channel estimation and tracking, there has emerged a trend of researchers increasingly considering the physics of the channel before to search for solutions in radio communications [3]–[6]. One of the physical phenomena of the underwater acoustic channel was demonstrated in [6]–[8], where it was shown that for many underwater acoustic channel impulse responses (CIRs),

The associate editor coordinating the review of this manuscript and approving it for publication was A. Taufiq Asyhari¹.

the multipath taps are correlated. This result may be due to the fluctuations of the water dividing the path into several similar paths. The signals may travel through a common region with similar sound speed variations. Additionally, the limitation of the channel bandwidth or bandwidth of the receivers and transmitters leads to the tap belonging to one path spreading to multiple adjacent taps [6].

The correlation characteristic of the underwater acoustic channels may potentially be used to improve the channel tracking since after certain decorrelation, the channel can become uncorrelated and may have a lower rank [9]. Even though some artificial intelligence (AI)-based protocols have been developed in recent studies of underwater acoustic communication and networking [10]–[12], they usually incur a high computational cost. However, based on the correlation characteristic, the performance can be improved and the computational cost can be reduced [9], [13], [14]. A model-based signal subspace channel tracking approach is proposed in [13]

for the correlated underwater acoustic channel. It is assumed that after decorrelation, the channel components become uncorrelated and slow-varying. A time-invariant autoregressive (AR) model with low order is used as the model for these uncorrelated channel components after decorrelation. This AR model has a simple form and can be used for the time evaluation of the channel components. Some experimental results support the conclusion that this AR model is reasonable for channel components [13], [14]. With this time-invariant AR model, a Kalman filter is used to track these channel components, thus realizing correlated underwater acoustic channel tracking. Based on this time-invariant AR model for channel components, adaptive subspace-tracking with reduced-rank model-based amplitude estimation (ASR-MAE) in [14] improves this channel tracking by adding a subspace tracker for the time variation of the subspace vector. An adaptive factor is introduced into the tracker in [15] to further improve the tracking ability.

However, model mismatch often happens in model-based underwater acoustic channel tracking since to date, no model has been able to fully describe the underwater acoustic channel. Once the channel components are not correlated and not evaluated in a time-invariant manner, the time-invariant AR model mismatches the channel components. Especially for the rapid time-varying underwater acoustic channel, this prior model mismatch is nonnegligible [16]. Thus, even though improved trackers can compensate for the mismatch to some degree [15], [16], a more tolerant model must be developed. The model itself needs to be tolerant to the occasionally uncorrelated channel components and time-variant evolutions, thereby improving the tracking performance in principle.

Based on the above considerations, the main contributions of this work are as follows:

- We propose a tolerant dynamic time-variant state-space model for the channel components in channel tracking. In the state-space model, we dynamically update the state-space model during the tracking process. Moreover, the model is tolerant to the model mismatch if the uncorrelated assumption for the channel components does not hold in the nonstationary underwater acoustic channel. Through this approach, we improve the state-space model for the rapid time-varying channel tracking.
- Moreover, a forward-backward Kalman filter is combined with the dynamic time-variant state-space model for rapid time-varying channel tracking named as dynamic forward-backward ASRMAE (DFB-ASRMAE). Since the rapid time-varying channel requires a high tracking ability, we provide the two-way tracker to improve tracking efficiency based on the proposed state-space model. Our results show that the proposed channel tracking decreases the normalized signal prediction error for rapid time-varying acoustic channels compared to the existing methods with the same experimental data.

II. SYSTEM MODEL

A. CORRELATED UNDERWATER ACOUSTIC CHANNELS

A time-varying underwater acoustic channel has M multipath arrivals that each have an amplitude $A_m(t)$ and arrival (delay) time $\tau_m(t)$:

$$c(\tau, t) = \sum_{m=1}^M A_m(t)\delta(\tau - \tau_m(t)), \quad (1)$$

where $c(\tau, t)$ is the channel impulse response at time t . Then, at the receiver, the effective CIR can be obtained:

$$h(\tau, t) = p_R(\tau) \otimes c(\tau, t) \otimes p_T(\tau), \quad (2)$$

where $p_R(\tau)$ and $p_T(\tau)$ are the receive filter and transmit filter, respectively. After sampling $h(\tau, t)$, we have $h_k(n) = h(\tau = kT_b, t = nT_g)$ for the k th tap at time n with $n = 1, 2, \dots, N$, where T_b is the duration of a symbol, given that the channel is acquired every T_g duration. Then, the CIR can be expressed in terms of a K -tap vector $\mathbf{h}(n) = [h_1(n), \dots, h_k(n), \dots, h_K(n)]^T$. For many underwater acoustic channels, the taps are found to be experimentally correlated [6], [7]. This is reasonable because many physical environments can make the taps correlated. The fluctuations of the water can divide the path into several similar paths. When many paths travel through a common region with similar sound speed variations, they may become correlated. Moreover, if the bandwidths of the receive filter and transmit filter are too narrow, the tap belonging to one path can easily spread to many adjacent taps [6].

The cross-path covariance matrix is given by $\mathbf{R}_h(n) = E[\mathbf{h}(n)\mathbf{h}^H(n)]$ where superscript H denotes the Hermitian conjugate. Through eigenvalue decomposition (EVD) of the covariance matrix,

$$\mathbf{R}_h(n) = \mathbf{Q}(n)\Lambda(n)\mathbf{Q}^H(n), \quad (3)$$

where $\mathbf{Q}(n)$ is a matrix of orthonormal eigenvectors, and $\Lambda(n)$ is a diagonal matrix of eigenvalues. Since channel taps are correlated, $\mathbf{R}_h(n)$ is ill-conditioned with assumed r -rank, where $r \ll K$. If the taps of the channel components in the eigenvector space after decomposition are uncorrelated [13] (we analyze this in Section V with experimental data), we have

$$\Lambda(n) = E[\mathbf{z}(n)\mathbf{z}^H(n)], \quad (4)$$

where $\mathbf{z}(n)$ are the channel components. The channel taps can be expressed as

$$\begin{aligned} \mathbf{h}(n) &= \mathbf{Q}(n)\mathbf{z}(n) \\ &= \mathbf{Q}_r(n)\mathbf{z}_r(n), \end{aligned} \quad (5)$$

where $\mathbf{z}_r(n) \in \mathbb{C}^{r \times 1}$ comprises the r largest channel components in $\mathbf{z}(n)$, and the eigenvectors associated with the r largest eigenvalues compose $\mathbf{Q}_r(n) \in \mathbb{C}^{K \times r}$ where $\mathbf{Q}_r^H(n)\mathbf{Q}_r(n) = \mathbf{I}_{r \times r}$.

It is obvious that if we can obtain $\mathbf{Q}_r(n)$ and $\mathbf{z}_r(n)$ at each state, then the underwater acoustic channel $\mathbf{h}(n)$ can be

tracked. Compared to $\mathbf{Q}_r(n)$, the channel principal components $\mathbf{z}_r(n)$ vary rapidly over time. To track the channel $\mathbf{h}(n)$, it is more important to track $\mathbf{z}_r(n)$. Therefore, in this work, we focus on the tracking of channel components $\mathbf{z}_r(n)$, with the tracked the channel subspace $\mathbf{Q}_r(n)$ according to [14].

B. AR MODEL TO THE CHANNEL PRINCIPLE COMPONENTS

To track the channel, we can use an AR model to describe the time evolution of the signal components $\mathbf{z}_r(n)$. Based on this model, the signal components $\mathbf{z}_r(n)$ are considered to follow a p -order discrete-time Markov process [17].

$$\mathbf{z}_r(n) = \sum_{l=1}^p \Phi(n, l) \mathbf{z}_r(n-l) + \boldsymbol{\eta}(n), \quad (6)$$

where $\Phi(n, l)$ is the l th-order state transition matrix at time n , and $\boldsymbol{\eta}(n)$ represents the process noise vector at time n and $\boldsymbol{\eta}(n) = [\eta_1(n), \eta_2(n), \dots, \eta_r(n)]^T$. Multiplying (6) by $\mathbf{z}_r^H(n-m)$ where $0 \leq m \leq p$ from the right side and taking expectation, we obtain

$$E[\mathbf{z}_r(n) \mathbf{z}_r^H(n-m)] = E[\boldsymbol{\eta}(n) \mathbf{z}_r^H(n-m)] + \sum_{l=1}^p \Phi(n, l) \times E[\mathbf{z}_r(n-l) \mathbf{z}_r^H(n-m)]. \quad (7)$$

If the taps of the signal components are uncorrelated, $E[z_i(n) z_j^*(l)] = R_i(n-l) \delta_{ij}$, where $z_i(n)$ represents the i th tap of $\mathbf{z}_r(n)$, $R_i(n-l) = E[z_i(n) z_i^*(l)]$ and is the autocorrelation of tap i component. Given that $\eta_i(n)$ and $z_j(n-m)$ are independent random variables,

$$E[\eta_i(n) z_i^*(n-m)] = \sum_{l=1}^p \Phi_i(n, l) E[\eta_i(n) z_i^*(n-m-l)] + E[\eta_i(n) \eta_i^*(n-m)] = R_{\eta_i} \delta(m), \quad (8)$$

where $R_{\eta_i} = E[\eta_i(n) \eta_i^*(n)]$ and is the process noise variance corresponding to the i th tap. Thus, (7) for the i th tap can be expressed as [13], [14]

$$R_i(m) = \sum_{l=1}^p \Phi_i(n, l) R_i(m-l) + R_{\eta_i} \delta(m) \quad i=1, 2, \dots, r. \quad (9)$$

The Yule-Walker equation can help us find the AR coefficients $\Phi_i(n, l)$.

III. CONVENTIONAL ASRMAE SUBSPACE CHANNEL TRACKING

The following conventional ASRMAE subspace channel tracking is taken from [13]–[15]. In conventional subspace channel tracking, the state transition coefficient $\Phi_i(n, l) = \phi_i(l)$ and is assumed to be time invariant. The channel principal components are modeled as an AR process (6), and a Kalman filter recursively tracks the channel components

based on this AR model. The state-space and the observation models in the Kalman filter are as follows:

$$\mathbf{Z}(n) = \Phi_z \mathbf{Z}(n-1) + \boldsymbol{\eta}_*(n), \quad (10)$$

$$r(n) = \mathbf{D}(n) \mathbf{Z}(n) + v(n), \quad (11)$$

where $\mathbf{Z}(n) = [\mathbf{z}_r^T(n), \dots, \mathbf{z}_r^T(n-p+1)]^T$, $\boldsymbol{\eta}_*(n) = [\boldsymbol{\eta}^T(n), \mathbf{0}_{1 \times r(p-1)}]^T$ and is the process noise vector assumed to be uncorrelated with each tap, and the state transition matrix Φ_z is denoted by

$$\Phi_z = \begin{bmatrix} \Phi(1) & \Phi(2) & \dots & \Phi(p) \\ \mathbf{I}_r & \mathbf{0}_r & \dots & \mathbf{0}_r \\ \vdots & \ddots & \ddots & \vdots \\ \mathbf{0}_r & \dots & \mathbf{I}_r & \mathbf{0}_r \end{bmatrix}, \quad (12)$$

where $\Phi(1) = \text{diag}([\phi_1(1), \phi_2(1), \dots, \phi_r(1)])$ and is the first-order state transition matrix with time-invariant assumption. The state-space model (10) in the Kalman filter is obtained by a rearranged (6) with time-invariant state transition coefficients. In the observation model (11), the received signal $r(n)$ can be expressed as $r(n) = \mathbf{d}(n)^T \mathbf{h}(n) + v(n)$, where $\mathbf{d}(n) = [d(n), d(n-1), \dots, d(n-K)]^T$ and is the transmitted data vector, and $v(n)$ is the observation noise, which is additive Gaussian white noise. $\mathbf{d}_z(n)^T = \mathbf{d}(n)^T \mathbf{Q}_r(n)$, and is the projection of the transmitted data vector on the signal subspace. Additionally, $\mathbf{D}(n) = [\mathbf{d}_z(n)^T, \mathbf{0}_{1 \times r(p-1)}]$.

To achieve the Kalman filter with (10) and (11) to track the channel components $\mathbf{z}_r(n)$, we need to estimate the state transition matrix Φ_z and process noise variance \mathbf{R}_η [14].

A. ESTIMATION OF STATE TRANSITION MATRIX Φ_z

Since the state transition coefficients are assumed to be time invariant, we convert $\{R_i(m)\}_{m=1}^p$ into a vector form as $\mathbf{R}_i = [R_i(1), R_i(2), \dots, R_i(p)]^T$, then (9) can be transformed into

$$\mathbf{R}_i = \underbrace{\begin{bmatrix} R_i(0) & R_i(-1) & \dots & R_i(-p+1) \\ R_i(1) & R_i(0) & \dots & R_i(-p+2) \\ \vdots & \ddots & \ddots & \vdots \\ R_i(p-1) & R_i(p-2) & \dots & R_i(0) \end{bmatrix}}_{\mathbf{r}_i} \times \underbrace{\begin{bmatrix} \phi_i(1) \\ \phi_i(2) \\ \vdots \\ \phi_i(p) \end{bmatrix}}_{\boldsymbol{\phi}_i}. \quad (13)$$

(13) is known as the Yule-Walker equation, and then, the state transition coefficients for the i th tap can be obtained as

$$\Phi_i = \mathbf{r}_i^{-1} \mathbf{R}_i. \quad (14)$$

It is clear that the state transition matrix Φ_z in (10) can be obtained by reshaping Φ_i as (12).

According to (13) and (14), to estimate Φ_i , it is necessary to first estimate $R_i(m)$. However, due to the lack of prior information about the channel principle components, we resort to using the least mean square (LMS) method for a coarse estimation of the CIR in (5), and then, we can obtain the channel components $\mathbf{z}_r(n)$.

We denote $\hat{\mathbf{h}}^{\text{LMS}}(n)$ as the estimated CIR at time n by LMS. The estimation error in LMS can be expressed as

$e(n) = r(n) - (\hat{\mathbf{h}}^{\text{LMS}})^H(n)\mathbf{d}(n)$. Then, iteratively, we can roughly estimate the channel by LMS as follows:

$$\hat{\mathbf{h}}^{\text{LMS}}(n+1) = \hat{\mathbf{h}}^{\text{LMS}}(n) + 2\mu e(n)\mathbf{d}(n), \quad (15)$$

where μ is the step factor. The estimated time-invariant cross-correlation matrix of channel is given by

$$\hat{\mathbf{R}}_h = \frac{1}{N_p} \sum_{n=1}^{N_p} \hat{\mathbf{h}}^{\text{LMS}}(n)(\hat{\mathbf{h}}^{\text{LMS}})^H(n), \quad (16)$$

where N_p is the length of the training sequence. Through EVD as described in (3), we can obtain the eigenvectors $\hat{\mathbf{Q}}_r(n)$ corresponding to the r largest eigenvalues. A rough estimation of the channel components can be obtained by projecting the $\hat{\mathbf{h}}^{\text{LMS}}(n)$ onto $\hat{\mathbf{Q}}_r(n)$ according to (5), $\hat{\mathbf{z}}_r^{\text{LMS}}(n) = \hat{\mathbf{Q}}_r^H(n)\hat{\mathbf{h}}^{\text{LMS}}(n)$. With $\hat{\mathbf{z}}_r^{\text{LMS}}(n)$, we have

$$\hat{R}_i(m) = \frac{1}{N_p} \sum_{n=1}^{N_p} \hat{z}_i^{\text{LMS}}(n)(\hat{z}_i^{\text{LMS}})^*(n-m). \quad (17)$$

After we obtain $\hat{R}_i(m)$, we can find \mathbf{R}_i and \mathbf{r}_i as in (13). Then, with (14), Φ_i can be estimated. Therefore, we can arrive at the state transition matrix Φ_z .

B. ESTIMATION OF PROCESS NOISE VARIANCE \mathbf{R}_η

The conventional estimation of \mathbf{R}_η is based on the assumption that the channel components of different taps $\mathbf{z}(n)$ are uncorrelated.

Letting $m = 0$ in (9), with the time-invariant state transition coefficient $\phi_i(l)$, we have

$$R_i(0) = \sum_{l=1}^p \phi_i(l)R_i(0-l) + R_{\eta,i}, \quad i=1, 2, \dots, r. \quad (18)$$

Since $R_i(m)$ can be estimated from (17) and $\phi_i(l)$ can be obtained from (14), $R_{\eta,i} = R_i(0) - \sum_{l=1}^p \phi_i(l)R_i(0-l)$.

By assuming that the channel components of different taps $\mathbf{z}(n)$ are uncorrelated as in (4), the left and right sides of (7) should be diagonal matrices, and the process noise is uncorrelated with different taps. Then, according to (7), (8) and (18), the noise variance matrix \mathbf{R}_η is a diagonal matrix and can be expressed as

$$\mathbf{R}_\eta = \text{diag}([R_{\eta,1}, R_{\eta,2}, \dots, R_{\eta,r}]). \quad (19)$$

IV. DYNAMIC FORWARD-BACKWARD SUBSPACE CHANNEL TRACKING FOR A RAPIDLY TIME-VARYING UNDERWATER ACOUSTIC CHANNEL

In this section, we propose a dynamic forward-backward subspace channel tracking method. We first provide a time-variant state-space model. In the time-variant state-space model, we update the state transition matrix dynamically and provide a new estimation of process noise statistics. The model mismatch due to the fast time-varying channel can be effectively mitigated. Then, to further adjust the time-varying property, a forward-backward Kalman filter

is combined with the dynamic state-space model as the proposed DFB-ASRMAE.

A. DYNAMIC MODEL ESTIMATION FOR A RAPIDLY TIME-VARYING CHANNEL

The proposed dynamic state-space model is as follows:

$$\mathbf{Z}(n) = \Phi_z(n)\mathbf{Z}(n-1) + \eta_*(n). \quad (20)$$

Different from (10), we assume that $\Phi_z(n)$ changes with time n in (20), and $\eta_*(n)$ is correlated with taps due to the model-mismatch in the rapidly time-varying channel. Thus, we can still use a low-order AR model to adapt to the rapidly time-varying channel.

1) DYNAMICALLY UPDATING THE STATE TRANSITION MATRIX FOR A RAPIDLY TIME-VARYING CHANNEL

Here, we introduce a dynamically updated state transition matrix $\Phi_z(n)$ in (20) based on the state-space model (20) and (11).

We first obtain the initial $\Phi_z(0) = \Phi_z$ with the conventional method as in Section III. A. Then, we use the following algorithm to update the state transition matrix every T_g duration based on the Kalman filter. The Kalman filter includes two main steps: update and prediction [18].

• Update

$$g(n) = \mathbf{D}(n)\hat{\mathbf{K}}(n, n-1)\mathbf{D}^H(n) + \sigma_v^2, \quad (21)$$

$$\mathbf{G}(n) = \hat{\mathbf{K}}(n, n-1)\mathbf{D}^H(n)g(n)^{-1}, \quad (22)$$

$$\xi(n) = r(n) - \mathbf{D}(n)\hat{\mathbf{Z}}(n, n-1), \quad (23)$$

$$\hat{\mathbf{Z}}(n, n) = \hat{\mathbf{Z}}(n, n-1) + \mathbf{G}(n)\xi(n), \quad (24)$$

$$\hat{\mathbf{K}}(n, n) = \hat{\mathbf{K}}(n, n-1) - \mathbf{G}(n)\mathbf{D}(n)\hat{\mathbf{K}}(n, n-1), \quad (25)$$

• Prediction

$$\hat{\mathbf{Z}}(n+1, n) = \Phi_z(n)\hat{\mathbf{Z}}(n, n), \quad (26)$$

$$\hat{\mathbf{K}}(n+1, n) = \Phi_z(n)\hat{\mathbf{K}}(n, n)\Phi_z^H(n) + \mathbf{R}_\eta, \quad (27)$$

where $\hat{\mathbf{Z}}(n, n) = [\hat{\mathbf{z}}_1^T(n), \dots, \hat{\mathbf{z}}_r^T(n-p+1)]^T$ and is the estimated state vector with the estimated channel components, σ_v^2 represents the variance of the observation noise, and $\Phi_z(n)$ is the state transition matrix at time n , which changes with time. In the update step, given the state vector $\hat{\mathbf{Z}}(n, n-1)$ and the Kalman error covariance matrix $\hat{\mathbf{K}}(n, n-1)$ predicted at the previous moment, we can obtain the Kalman gain $\mathbf{G}(n)$ and the signal prediction error $\xi(n)$. In the prediction step, the predicted state vector $\hat{\mathbf{Z}}(n+1, n)$ and predicted covariance matrix $\hat{\mathbf{K}}(n+1, n)$ are obtained.

To predict the state transition matrix $\Phi_z(n+1)$, we extract $\hat{z}_i(n+1)$ from the predicted state vector $\hat{\mathbf{Z}}(n+1, n)$. The predicted channel component autocorrelation for the i th tap is as follows:

$$\begin{aligned} \hat{R}_i(m, n+1) &= \frac{1}{n+1} \sum_{l=1}^{n+1} \hat{z}_i(l)\hat{z}_i^*(l-m) \\ &= \frac{n}{n+1} \hat{R}_i(m, n) \\ &\quad + \frac{1}{n+1} \hat{z}_i(n+1)\hat{z}_i^*(n+1-m), \end{aligned} \quad (28)$$

where $\hat{R}_i(m, n)$ is time variant $\hat{R}_i(m)$, and $\hat{R}_i(m, n)$ is estimated with the data obtained before time n , rather than N_p as used in (17) for $\hat{R}_i(m)$. With $\hat{R}_i(m, n + 1)$, we can obtain the predicted state transition matrix $\Phi_z(n + 1)$ according to (14).

For many underwater acoustic channels, especially rapidly time-varying channels, the model time variation is not negligible. The conventional time-invariant state transition matrix can lead to accumulative mismatch for the state-space model. By contrast, the proposed dynamically updated state transition matrix can lower such mismatch.

2) CORRELATED PROCESS NOISE COVARIANCE ESTIMATION

For the conventional state-space model, it is assumed that after EVD, the subspaces corresponding to the channel components are orthogonal to each other, and the channel components are uncorrelated; therefore, the noise in state-space should be uncorrelated. However, for the fast-varying channel, after decorrelation, the channel components may still be slightly correlated since the channel changes quickly. Then, the process noise becomes correlated. The diagonal assumption about the R_η in (19) no longer holds.

With the conventional method in Section III. A, we can obtain $\Phi_z(0)$ and the rough channel components $\hat{z}_r^{LMS}(n)$. Then, with $\hat{\Phi}(l)$ extracted from $\Phi_z(0)$ and $\hat{z}_r^{LMS}(n)$, we can estimate the process noise vector based on (6) as follows:

$$\hat{\eta}(n) = \hat{z}_r^{LMS}(n) - \sum_{l=1}^p \hat{\Phi}(l)\hat{z}_r^{LMS}(n-l). \tag{29}$$

Then, for the correlated process noise, the estimated covariance of the process noise \hat{R}_η is given by

$$\hat{R}_\eta = \frac{1}{N_p} \sum_{n=1}^{N_p} \hat{\eta}(n)\hat{\eta}^H(n), \tag{30}$$

where N_p is the time-length of the training data. Compared with the conventional method, \hat{R}_η is no longer a diagonal matrix. It can help the state-space model to adapt to the fast-varying underwater acoustic channel tracking. \hat{R}_η does not need to be updated at every time state.

B. FORWARD-BACKWARD KALMAN FILTER FOR CHANNEL TRACKING

In this section, to further improve the channel tracking, we combine the dynamically updated state-space model proposed above with forward-backward Kalman filtering [19], [20] as DFB-ASRMAE. The forward-backward Kalman filter can better adapt to the time-variant state-space model. The forward-backward Kalman filtering includes three steps: forward filtering, backward filtering, and optimal joint estimation.

In the backward filtering, different from the conventional Kalman filter tracking along time $n = 1$ to N as the forward tracking, the backward Kalman filter recursively tracks from

time $n = N$ back to 1. Since $\Phi(n)$ is a nonsingular diagonal matrix, multiplying the conventional state model (20) by $\Phi^{-1}(n)$ on the left, we have:

$$\Phi^{-1}(n)\mathbf{Z}(n) = \mathbf{Z}(n-1) + \Phi^{-1}(n)\eta(n). \tag{31}$$

Then, we have the backward Kalman filter with the backward state-space model and the observation model as follows

$$\mathbf{Z}(n-1) = \Phi_b(n)\mathbf{Z}(n) + \eta_b(n), \tag{32}$$

$$r(n) = \mathbf{D}(n)\mathbf{Z}(n) + v(n), \tag{33}$$

where subscript b represents the parameters for the backward Kalman filter. Clearly, the state transition matrix and the process noise can be obtained as $\Phi_b(n) = \Phi^{-1}(n)$ and $\eta_b(n) = \Phi^{-1}(n)\eta(n)$, respectively. Then, backward Kalman filtering can similarly apply the sequential procedure in Kalman filtering, from time $n = N$ back to 1.

To explain the forward-backward Kalman filter for the channel tracking, here, we simplify the forward system (20)(11) and the backward system (32)(33) as follows:

$$r_f(n) = \mathbf{D}_f(n)\mathbf{Z}(n) + v_f(n), \tag{34}$$

$$r_b(n) = \mathbf{D}_b(n)\mathbf{Z}(n) + v_b(n), \tag{35}$$

where $\mathbf{Z}(n)$ is to be estimated, $r_f(n)$ and $r_b(n)$ are the outputs of the forward and backward systems, $\mathbf{D}_f(n)$ and $\mathbf{D}_b(n)$ represent the system matrix, and $v_f(n)$ and $v_b(n)$ represent the observation noise vectors. Since Kalman filtering is a generalization of sequential linear minimum mean square estimation (LMMSE), we study the LMMSE of $\hat{\mathbf{Z}}_f(n)$ for the forward system:

$$\begin{aligned} \hat{\mathbf{Z}}_f(n) &= \left(\mathbf{R}_z^{-1} + \mathbf{D}_f^H(n)\mathbf{D}_f(n)/\sigma_{vf}^2 \right)^{-1} \mathbf{D}_f^H(n)r_f(n)/\sigma_{vf}^2 \\ &= \mathbf{M}_f(n)\mathbf{D}_f^H(n)r_f(n)/\sigma_{vf}^2, \end{aligned} \tag{36}$$

where \mathbf{R}_z is the covariance of $\mathbf{Z}(n)$, and σ_{vf}^2 is the variance of $v_f(n)$. $\mathbf{M}_f(n)$ represents the estimation error matrix of $\hat{\mathbf{Z}}_f(n)$. Similar to (36), the LMMSE of $\hat{\mathbf{Z}}_b(n)$ obtained from the backward system can be expressed as

$$\hat{\mathbf{Z}}_b(n) = \mathbf{M}_b(n)\mathbf{D}_b^H(n)r_b(n)/\sigma_{vb}^2. \tag{37}$$

Combining the linear system (34) with (35), we have

$$\underbrace{\begin{bmatrix} r_f(n) \\ r_b(n) \end{bmatrix}}_{\tilde{\mathbf{r}}(n)} = \underbrace{\begin{bmatrix} \mathbf{D}_f(n) \\ \mathbf{D}_b(n) \end{bmatrix}}_{\tilde{\mathbf{D}}(n)} \mathbf{Z}(n) + \underbrace{\begin{bmatrix} v_f(n) \\ v_b(n) \end{bmatrix}}_{\tilde{\mathbf{v}}(n)}, \tag{38}$$

where $\mathbf{C}_{\tilde{\mathbf{v}}} = \text{diag}([\sigma_{vf}^2, \sigma_{vb}^2])$ and is the covariance of $\tilde{\mathbf{v}}(n)$. In estimation theory, the estimation can be improved with more informational data [21]. While the forward and backward systems are not fully independent, the combined system provides more information than either the forward system or backward system only. Therefore, the estimation from the combined approach (38) should be better than that from

TABLE 1. Channel Tracking Algorithm DFB-ASRMAE.

Initialization	No. of operations
Obtain the rough channel estimation $\hat{\mathbf{h}}^{\text{LMS}}(n)$ by LMS;	
Let $\mathbf{z}_r^{\text{LMS}}(n) = \mathbf{Q}_r^H(n)\hat{\mathbf{h}}^{\text{LMS}}(n)$;	
Estimate $\Phi_z(0)$ according to Section III. A and set the initial value of $\sigma_{v_f}^2, \sigma_{v_b}^2$; // Initialize the state transition matrix	
Estimate the process noise covariance $\hat{\mathbf{R}}_\eta$ according to (29)(30); //Estimate the process noise statistics	
For $n = 1, 2, \dots, N$ //Forward tracking	
Track signal subspace $\mathbf{Q}_r(n)$ by PASTd [22];	$O(4Kr)$
(21)(22)(23)(33)(25) to obtain $\hat{\mathbf{Z}}(n, n)$ and $\mathbf{K}(n, n)$; // Update in forward Kalman filter	
(26)(27) to obtain $\hat{\mathbf{Z}}(n+1, n)$ and $\mathbf{K}(n+1, n)$; //Prediction in the forward Kalman filter	$O(3(rp)^3)$
if $n < N_p$ // Predict $\Phi(n)$	
$\Phi_z(n+1) = \Phi_z(0)$;	
else	
Extract $\hat{z}_i(n+1)$ from $\hat{\mathbf{Z}}(n+1, n)$ and obtain $\hat{R}_i(m, n+1)$ by (28);	$O(p)$
Substitute $\hat{R}_i(m, n+1)$ into (14) to estimate $\Phi_i(n+1)$ and then obtain $\Phi(n+1)$;	$O(p^2 + p^3)$
end	
End	
For $n = N, N-1, \dots, 1$ // Backward tracking	
Set $\Phi_b(0) = \Phi_z^{-1}(0), \Phi_b(n) = \Phi_z^{-1}(n)$ and $\hat{\mathbf{R}}_{\eta b} = \Phi_b(N)\hat{\mathbf{R}}_\eta\Phi_b(N)^H$;	$O((rp)^3)$
Update the backward Kalman filter to obtain $\hat{\mathbf{Z}}_b(n, n)$ and $\mathbf{K}_b(n, n)$;	
Prediction in the backward Kalman Filter to obtain $\hat{\mathbf{Z}}_b(n-1, n)$ and $\mathbf{K}_b(n-1, n)$;	$O(3(rp)^3)$
End	
Tracking output	
(42) to obtain $\tilde{\mathbf{M}}(n, n)$ with $\mathbf{K}(n, n)$ and $\mathbf{K}_b(n, n)$;	$O(3(rp)^3)$
(43) to obtain combining optimal $\tilde{\mathbf{Z}}(n)$ with $\mathbf{K}(n, n), \mathbf{K}_b(n, n)$ and $\hat{\mathbf{Z}}(n, n), \hat{\mathbf{Z}}_b(n, n)$;	$O(3(rp)^2)$
$\hat{\mathbf{h}}_{\text{DFB-ASRMAE}}(n) = \mathbf{Q}_r(n)\tilde{\mathbf{Z}}(n)$; //Tracked channel with DFB-ASRMAE	$O(Kr)$
$\xi_{\text{DFB-ASRMAE}}(n) = r(n) - \mathbf{D}(n)\tilde{\mathbf{Z}}(n)$. //Signal prediction error	
End	
Total complexity: $O(\max(6Kr, 10(rp)^3))$	

simple forward or backward filtering. The LMMSE of $\mathbf{Z}(n)$ for (38) is

$$\begin{aligned} \tilde{\mathbf{Z}}(n) &= (\mathbf{R}_z^{-1} + \tilde{\mathbf{D}}^H(n)\mathbf{C}_v^{-1}\tilde{\mathbf{D}}(n)\tilde{\mathbf{D}}^H(n)\mathbf{C}_v^{-1})^{-1}\tilde{\mathbf{r}}(n) \\ &= \left(\mathbf{R}_z^{-1} + \mathbf{D}_f^H(n)\mathbf{D}_f(n)/\sigma_{v_f}^2 + \mathbf{D}_b^H(n)\mathbf{D}_b(n)/\sigma_{v_b}^2\right)^{-1} \\ &\quad \times \left(\mathbf{D}_f^H(n)r_f(n)/\sigma_{v_f}^2 + \mathbf{D}_b^H(n)r_b(n)/\sigma_{v_b}^2\right) \\ &= \left(\mathbf{M}_f^{-1}(n) + \mathbf{M}_b^{-1}(n) - \mathbf{R}_z^{-1}\right)^{-1} \\ &\quad \times \left(\mathbf{D}_f^H(n)r_f(n)/\sigma_{v_f}^2 + \mathbf{D}_b^H(n)r_b(n)/\sigma_{v_b}^2\right) \\ &= \tilde{\mathbf{M}}(n) \left(\mathbf{D}_f^H(n)r_f(n)/\sigma_{v_f}^2 + \mathbf{D}_b^H(n)r_b(n)/\sigma_{v_b}^2\right). \end{aligned} \quad (39)$$

Therefore, the relationship between $\hat{\mathbf{Z}}_f(n), \hat{\mathbf{Z}}_b(n)$ and $\tilde{\mathbf{Z}}(n)$ is as follows:

$$\tilde{\mathbf{M}}^{-1}(n)\tilde{\mathbf{Z}}(n) = \mathbf{M}_f^{-1}(n)\hat{\mathbf{Z}}_f(n) + \mathbf{M}_b^{-1}(n)\hat{\mathbf{Z}}_b(n), \quad (40)$$

$$\tilde{\mathbf{M}}^{-1}(n) = \mathbf{M}_f^{-1}(n) + \mathbf{M}_b^{-1}(n) - \mathbf{R}_z^{-1}(n), \quad (41)$$

where \mathbf{R}_z can be omitted in order to simplify the problem. $\hat{\mathbf{Z}}_f(n) = \hat{\mathbf{Z}}(n, n)$ as in (33). For LMMSE, the error covariance $\tilde{\mathbf{M}}(n), \mathbf{M}_f(n)$ and $\mathbf{M}_b(n)$ are also MSEs, and therefore, $\mathbf{M}_f(n) = \mathbf{K}(n, n)$, and $\mathbf{M}_b(n) = \mathbf{K}_b(n, n)$. Then, for forward-backward Kalman filtering, a refined estimate $\tilde{\mathbf{Z}}(n)$ at time n is as follows:

$$\tilde{\mathbf{M}}(n) = \left(\mathbf{K}^{-1}(n, n) + \mathbf{K}_b^{-1}(n, n)\right)^{-1}, \quad (42)$$

$$\tilde{\mathbf{Z}}(n) = \tilde{\mathbf{M}}(n) \left(\mathbf{K}^{-1}(n, n)\hat{\mathbf{Z}}(n, n) + \mathbf{K}_b^{-1}(n, n)\hat{\mathbf{Z}}_b(n, n)\right). \quad (43)$$

Then, $\tilde{\mathbf{Z}}(n)$ in (43) after the forward-backward Kalman filter contains the final tracked channel components. $\hat{\mathbf{h}}_{\text{DFB-ASRMAE}}(n) = \mathbf{Q}_r(n)\tilde{\mathbf{Z}}(n)$, and is the tracked channel with the proposed DFB-ASRMAE algorithm. The detailed steps of DFB-ASRMAE algorithm are given in Table 1, and the algorithm has a complexity on the order of $O(\max(6Kr, 10(rp)^3))$. Note that the ASRMAE algorithm has a computation complexity on the order of $O(\max(6Kr, 3(rp)^3))$ [14]. To obtain (43), we need parameters from forward filtering and backward filtering. Hence, in the algorithm, we carry out forward filtering, backward filtering, and then the optimal joint estimation, as shown in Table 1.

V. EXPERIMENTAL RESULTS

The 2007 Autonomous Underwater Vehicle Festival (AUVFest07) experiment acoustic communication data previously studied in [8], [13], [14] are used to verify our proposed channel tracking algorithm. The experiment was conducted in 20 m of coastal water under relatively calm and rough sea conditions. Since the source and receiver are mounted on the bottom of a rigid body, we do not need to consider the signal fluctuations due to the source or receiver's movement. The measured CIRs are shown in Fig. 1. The CIRs under both rough sea and calm sea are time variant due to internal waves. Furthermore, the CIRs in the rough sea are more rapidly time-varying than those in the calm sea. For both sea conditions, three to four dominant paths are clearly shown in Fig. 1, and the delay for each path does not belong to a single delay tap but rather spreads to multiple adjacent taps. This means that the channel taps are

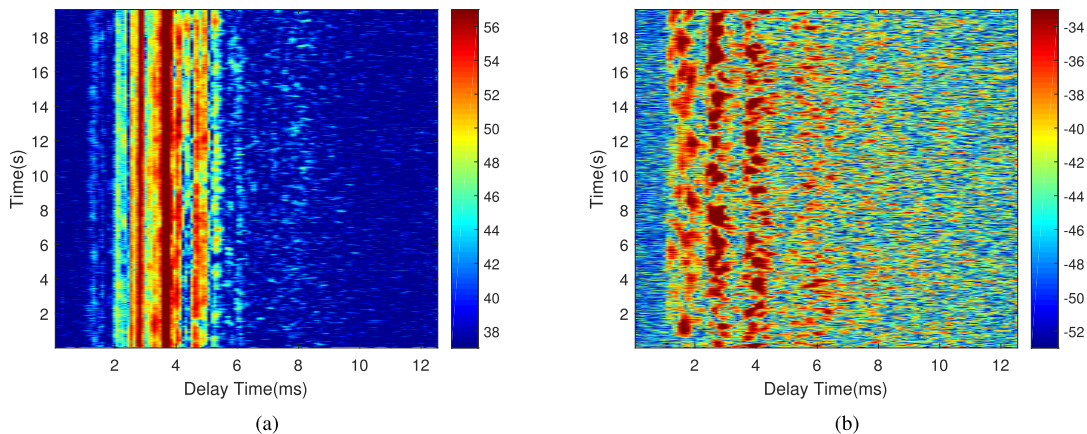


FIGURE 1. Measured CIRs for the AUVFest07 data under the calm sea (a) and the rough sea (b) [14].

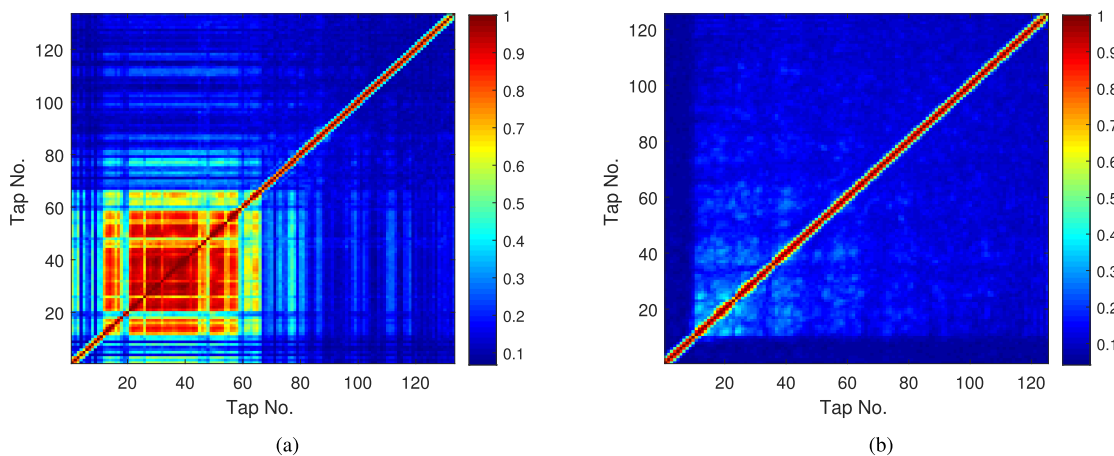


FIGURE 2. The cross-path coherence estimated for AUVFest07 in the calm sea (a) and the rough sea (b). The Tap No. refers to the k -th delay tap in $h_k(n)$ at time n .

correlated with respect to delay for both calm and rough seas.

The cross-path coherence [8] can be given by

$$p_h[j, k] = \frac{E \left[h_j^*(n) h_k(n) \right]}{\sqrt{E \left[|h_j(n)|^2 \right] E \left[|h_k(n)|^2 \right]}}, \quad (44)$$

where $E \left[|h_k(n)|^2 \right] = \frac{1}{N_p} \sum_{n=1}^{N_p} \hat{h}_k^*(n) \hat{h}_k(n)$, and $\hat{h}_k(n)$ corresponds to the estimated k -th delay tap of channel at time n . Fig. 2 shows the cross-path coherence in different sea conditions. Even in the rough sea, some off-diagonal elements still have magnitudes comparable to those of the diagonal elements. This means that the channel taps are correlated in both calm and rough sea conditions.

Due to the above correlation characteristic of the channel, we can use EVD to obtain eigenvalues $\Lambda(n)$. The normalized eigenvalue spectra for the two different sea conditions (in Fig. 1) are shown in Fig. 3. The eigenvalue drops rapidly from $k = 1$ to 10 and becomes stable between 11 to 20. This means that the rank of the channel subspace can be chosen as $11 \leq r \leq 20$. This is much smaller than the dimension of

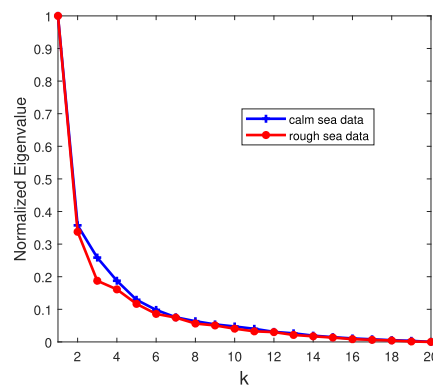


FIGURE 3. The normalized eigenvalues (k th diagonal element in $\Lambda(n)$) of the channel for the calm sea and the rough sea.

the CIR taps ($K \geq 100$). Moreover, the curves showing the decrease in the eigenvalues in the calm seas and rough seas are similar. Thus, we can choose the same r in different sea conditions.

We define a cross-path coherence for the channel principle components as follows, which is similar to the cross-path

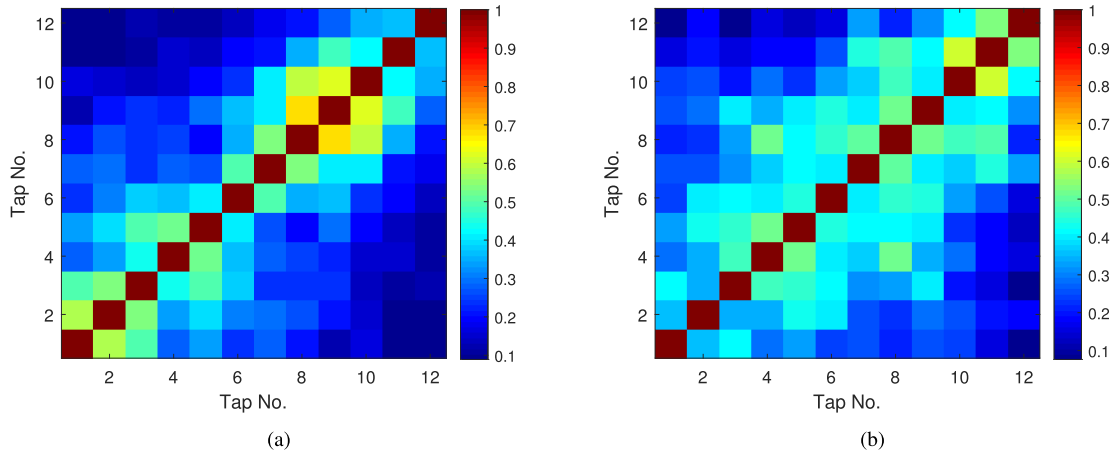


FIGURE 4. Cross-path coherence of the channel components with $p = 1$ and $r = 12$ for the calm sea (a) and the rough sea (b). Tap No. refers to i -th tap in $z_i(n)$ at time n .

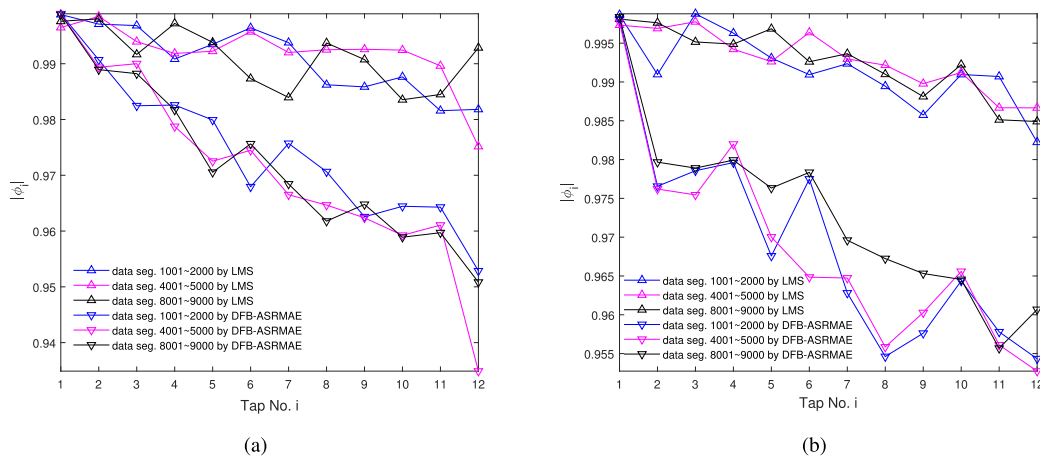


FIGURE 5. State transition coefficient $|\phi_i|$ for tap $i = 1, \dots, 12$, with $p = 1$ and $r = 12$ where z_i were estimated by LMS and DFB-ASRMAE algorithms with different data segments for the calm sea (a) and the rough sea (b).

coherence of a channel:

$$\rho_z[i, j] = \frac{E [z_i^*(n)z_j(n)]}{\sqrt{E [|z_i(n)|^2] E [|z_j(n)|^2]}}, \quad (45)$$

where $E [|z_i(n)|^2] = \frac{1}{N_p} \sum_{n=1}^{N_p} \hat{z}_i^*(n)\hat{z}_i(n)$, and $\hat{z}_i(n)$ corresponds to the estimated channel component of the i -th tap at time n . The cross-path coherence of the channel components is shown in Fig. 4. We observe that diagonal elements contain most of the power. It is reasonable that conventional channel tracking assumes that the channel components are generally uncorrelated for different taps. However, some of the off-diagonal elements have magnitudes comparable to those of the diagonal elements both in calm and rough sea conditions (the cross-path covariance matrix is not a strict diagonal matrix). Therefore, to compensate for the conventional assumption, we assume that the process noise is correlated in the space-time model.

To analyze the state transition matrix, here, we use a low-order state-space AR model with $p = 1$, and then, the state transition matrix becomes a diagonal matrix.

Figs. 5(a)-(b) show the state transition coefficients in the diagonal matrix obtained by the conventional method based on LMS as in Section III. A and the proposed DFB-ASRMAE under different sea conditions. The dynamically updated state transition coefficients obtained by DFB-ASRMAE are different from the conventional state transition coefficients. Moreover, the dynamically updated state transition coefficients in rough sea show more changes with different data time-segments. This observation suggests that the state transition coefficients are time variant at a certain level and that dynamically updating the state transition matrix can improve channel tracking in the rough sea more than in the calm sea.

To compare the conventional methods in [13]–[15], we continue to use the normalize signal prediction error as $|\xi(n)|^2/E|r(n)|^2$.

Figs. 6 (a) and (b) show the normalized signal prediction error tracked by ASRMAE [14], A-ASRMAE [15] and DFB-ASRMAE, separately, for the calm sea and rough sea conditions with the AUVFest07 data. To compare the performance of different algorithms, we set the same AR order

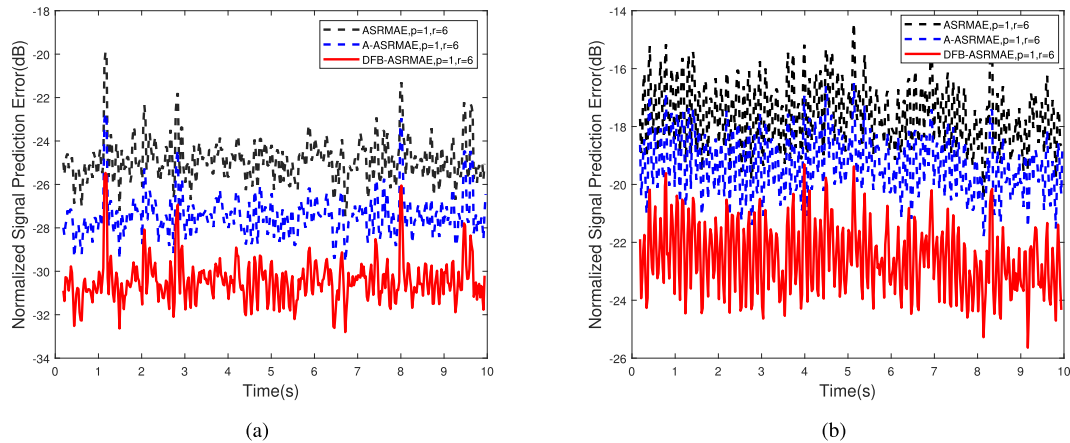


FIGURE 6. Comparison of normalized signal prediction error as a function of time using various channel tracking algorithms for AUVFest07 in calm sea (a) and in rough sea (b). The mean normalized signal prediction errors in the calm sea are -25.1 dB for ASRMAE, -27.4 dB for A-ASRMAE, and -30.4 dB for DFB-ASRMAE, as marked on the right vertical axis in (a). In the rough sea (b), the mean normalized signal prediction errors are -17.6 dB for ASRMAE, -19.3 dB for A-ASRMAE, and -22.6 dB for DFB-ASRMAE.

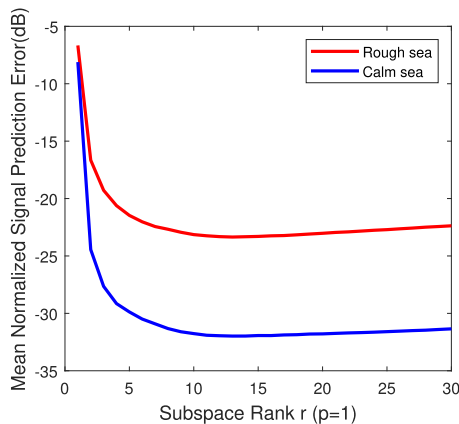


FIGURE 7. Mean normalized signal prediction error by DFB-ASRMAE as a function of r for the AUVFest07 data.

$p = 1$ and the same rank $r = 6$ as in [14], [15]. The mean normalized signal prediction errors for the calm sea data are -25.1 dB for ASRMAE, -27.4 dB for A-ASRMAE, and -30.4 dB for DFB-ASRMAE, as shown in Fig. 6(a). For the rough sea data, the mean normalized signal prediction errors are -17.6 dB for ASRMAE, -19.3 dB for A-ASRMAE and -22.6 dB for DFB-ASRMAE, as shown in Fig. 6(b).

The mean normalized signal prediction errors of A-ASRMAE and DFB-ASRMAE are lower than those of ASRMAE for both the calm sea and rough sea conditions. A-ASRMAE yields a mean 2.3 dB improvement in the calm sea and 1.7 dB improvement in the rough sea in the signal prediction error compared with the ASRMAE algorithm since it introduces an adaptive procedure to compensate for the mismatch of the tracking model. For the DFB-ASRMAE algorithm, the mean signal prediction error is the lowest among the three algorithms: under the setting $p = 1$ and $r = 6$, it is 5.3 dB and 5.0 dB lower than those obtained by ASRMAE for the calm sea conditions and the rough sea

conditions, respectively. DFB-ASRMAE adopts a dynamic time-variant space-time model with correlated tolerance. Therefore, it can improve the channel tracking performance in principle. Moreover, the forward-backward filtering can further help to track the channel with this time-variant model.

Furthermore, we discuss the parameter setting. Since higher-order p can give rise to a high complexity of DFB-ASRMAE, we set $p = 1$ in this work. We provide the tracking results of the DFB-ASRMAE algorithm with changing r under $p = 1$ in Fig. 7. The results show that the mean normalized prediction error reaches the lowest value at approximately $r = 12$ with the proposed DFB-ASRMAE for both the calm sea data and rough sea data. Based on the examination of Figs. 7 and 3, we can reach the same conclusion that it is reasonable to set the same rank r for different sea conditions.

Therefore, we set $p = 1$ and $r = 12$ for DFB-ASRMAE and compare it with TBA-ASRMAE [15] with the same AUVFest07 data. In TBA-ASRMAE, all of the parameters are set according to its training procedure, and the AR order and subspace rank are $p = 2$ and $r = 20$, respectively, and are the optimal parameters for TBA-ASRMAE in both calm seas and rough seas. Both show performance superior to those of ASRMAE and A-ASRMAE (see Fig. 6) with $p = 1$ and $r = 6$. DFB-ASRMAE yields a 2.9 dB improvement in the signal error prediction error in the calm sea and a 4.0 dB improvement in the rough sea compared with TBA-ASRMAE, which has a higher AR order and more subspaces. Furthermore, the DFB-ASRMAE shows more improvement in the rough sea than in the calm sea. Even though the rough channel changes strongly over time, the dynamical time-variant space-time model with correlated tolerance and a forward-backward Kalman filter in DFB-ASRMAE can work well together to track the channel's rapid changes.

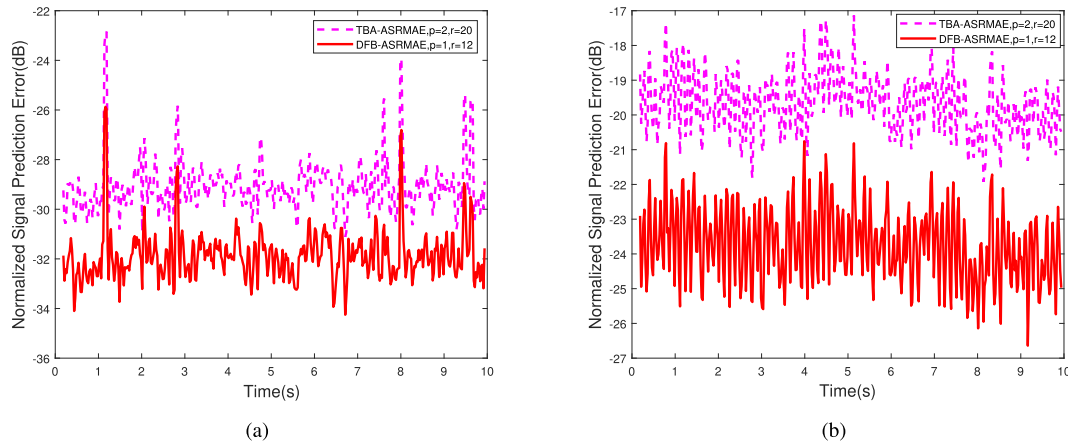


FIGURE 8. Comparison of the normalized signal prediction error as a function of time using various channel tracking algorithms for AUVFest07 in calm sea (a) and in rough sea (b). The mean normalized signal prediction errors for the calm sea data are -29.0 dB for TBA-ASRMAE ($p = 2, r = 20$) and -31.9 dB for DFB-ASRMAE ($p = 1, r = 12$). For the rough sea data (b), the mean normalized signal prediction errors for the rough sea data are 19.7 dB for TBA-ASRMAE ($p = 2, r = 20$) and -23.7 dB for DFB-ASRMAE ($p = 1, r = 12$).

VI. CONCLUSION

In this work, we consider the model mismatch problem for model-based channel tracking. The model is based on channel physics in that the underwater acoustic channel is correlated. In the model, the channel components are assumed to be uncorrelated with a time-invariant transaction after decorrelation. However, this assumption does not always hold for the real underwater acoustic channel. Therefore, we propose a dynamic state-space model that is more tolerant to the rapid time-varying channel for channel tracking. Furthermore, a forward-backward Kalman filter is combined with the dynamic state-space model, further improving the tracking performance. The proposed DFB-ASRMAE with only a 1-order AR model can decrease the normalized signal prediction error significantly with experimental data only.

ACKNOWLEDGMENT

The authors would like to thank Prof. T. C. Yang and Dr. X. Han for providing the AUVFest07 data.

REFERENCES

- [1] D. B. Kilfoyle and A. B. Baggeroer, "The state of the art in underwater acoustic telemetry," *IEEE J. Ocean. Eng.*, vol. 25, no. 1, pp. 4–27, Jan. 2000.
- [2] M. R. Khan, B. Das, and B. B. Pati, "Channel estimation strategies for underwater acoustic (UWA) communication: An overview," *J. Franklin Inst.*, vol. 357, no. 11, pp. 7229–7265, Jul. 2020.
- [3] A. Song, M. Stojanovic, and M. Chitre, "Editorial underwater acoustic communications: Where we stand and what is next?" *IEEE J. Ocean. Eng.*, vol. 44, no. 1, pp. 1–6, Jan. 2019.
- [4] C. R. Berger, S. Zhou, J. C. Preisig, and P. Willett, "Sparse channel estimation for multicarrier underwater acoustic communication: From subspace methods to compressed sensing," *IEEE Trans. Signal Process.*, vol. 58, no. 3, pp. 1708–1721, Mar. 2010.
- [5] X. Chen, W. Li, Q. Lu, P. Willett, and Q. Zhang, "Underwater acoustic channel tracking by multi-Bernoulli filter," in *Proc. OCEANS-MTS/IEEE Kobe Techno-Oceans (OTO)*, May 2018, pp. 1–8.
- [6] S. H. Huang, T. C. Yang, and C.-F. Huang, "Multipath correlations in underwater acoustic communication channels," *J. Acoust. Soc. Amer.*, vol. 133, no. 4, pp. 2180–2190, Apr. 2013.
- [7] R. Nadakuditi and J. C. Preisig, "A channel subspace post-filtering approach to adaptive least-squares estimation," *IEEE Trans. Signal Process.*, vol. 52, no. 7, pp. 1901–1914, Jul. 2004.
- [8] T. C. Yang, "Properties of underwater acoustic communication channels in shallow water," *J. Acoust. Soc. Amer.*, vol. 131, no. 1, pp. 129–145, Jan. 2012.
- [9] M. K. Tsatsanis, G. B. Giannakis, and G. Zhou, "Estimation and equalization of fading channels with random coefficients," in *Proc. IEEE Int. Conf. Acoust., Speech, Signal Process. Conf. Proc.*, Atlanta, GA, USA, vol. 2, Dec. 1996, pp. 1093–1096.
- [10] Z. Jin, Q. Zhao, and Y. Su, "RCAR: A reinforcement-learning-based routing protocol for congestion-avoided underwater acoustic sensor networks," *IEEE Sensors J.*, vol. 19, no. 22, pp. 10881–10891, Nov. 2019.
- [11] Y. Chen, J. Zhu, L. Wan, S. Huang, X. Zhang, and X. Xu, "ACOA-AFSA fusion dynamic coded cooperation routing for different scale multi-hop underwater acoustic sensor networks," *IEEE Access*, vol. 8, pp. 186773–186788, 2020.
- [12] M. S. M. Alamgir, M. N. Sultana, and K. Chang, "Link adaptation on an underwater communications network using machine learning algorithms: Boosted regression tree approach," *IEEE Access*, vol. 8, pp. 73957–73971, 2020.
- [13] S. H. Huang, J. Tsao, T. C. Yang, and S.-W. Cheng, "Model-based signal subspace channel tracking for correlated underwater acoustic communication channels," *IEEE J. Ocean. Eng.*, vol. 39, no. 2, pp. 343–356, Apr. 2014.
- [14] S. H. Huang, T. C. Yang, and J. Tsao, "Improving channel estimation for rapidly time-varying correlated underwater acoustic channels by tracking the signal subspace," *Ad Hoc Netw.*, vol. 34, pp. 17–30, Nov. 2015.
- [15] X. Wang, W. Li, Y. Liu, and Y. Chen, "Training-based adaptive channel tracking for correlated underwater acoustic channels," in *Proc. Int. Conf. Underwater Netw. Syst.*, Oct. 2019, pp. 1–5.
- [16] Y. Wang, J. Tao, L. Yang, F. Yu, C. Li, and X. Han, "Improved model-based channel tracking for underwater acoustic communications," in *Proc. IEEE 11th Sensor Array Multichannel Signal Process. Workshop (SAM)*, Hangzhou, China, Jun. 2020, pp. 1–5.
- [17] M. K. Tsatsanis, G. B. Giannakis, and G. Zhou, "Estimation and equalization of fading channels with random coefficients," *Signal Process.*, vol. 53, nos. 2–3, pp. 211–229, Sep. 1996.
- [18] R. E. Kalman, "A new approach to linear filtering and prediction problems," *J. Basic Eng.*, vol. 82, no. 1, pp. 35–45, Mar. 1960.
- [19] M. Bashir, D. Truhachev, and C. Schlegel, "Kalman forward-backward channel tracking and combining for OFDM in underwater acoustic channels," in *Proc. OCEANS-MTS/IEEE Kobe Techno-Oceans (OTO)*, May 2018, pp. 1–10.
- [20] S. Wang, Z. He, K. Niu, P. Chen, and Y. Rong, "New results on joint channel and impulsive noise estimation and tracking in underwater acoustic OFDM systems," *IEEE Trans. Wireless Commun.*, vol. 19, no. 4, pp. 2601–2612, Apr. 2020.
- [21] S. M. Kay, *Fundamentals of Statistical Signal Processing, Volume I: Estimation Theory*. Upper Saddle River, NJ, USA: Prentice-Hall, 1998.
- [22] B. Yang, "Projection approximation subspace tracking," *IEEE Trans. Signal Process.*, vol. 43, no. 1, pp. 95–107, Jan. 1995.



QIHANG HUANG received the B.S. degree in electronic and information engineering from the Harbin Institute of Technology, Harbin, China, in 2019. He is currently pursuing the M.S. degree in electronics and communication engineering with the Harbin Institute of Technology, Shenzhen, China. His research interests include underwater acoustic communication, algorithm design, and channel tracking.



YUHANG WANG received the B.S. degree in communication engineering from the Harbin Institute of Technology, Shenzhen, in 2020. She is currently pursuing the M.S. degree with the Harbin Institute of Technology. Her current research interests include underwater acoustic communication and underwater acoustic channel tracking.



WEI LI (Member, IEEE) received the B.S. degree in electric and information engineering from the Dalian University of Technology, Dalian, China, in 2004, and the Ph.D. degree in signal and information processing from the Institute of Acoustics, Chinese Academy of Sciences, Beijing, China, in 2009. From September 2015 to October 2016, she visited the University of Connecticut, Storrs, CT, USA. She is currently an Associate Professor with the School of Electric and Information Engineering, Harbin Institute of Technology, Shenzhen. Her research interests include underwater acoustic communication, underwater acoustic detection and estimation, statistical signal processing, and wireless communications.



WEICHENG ZHAN received the B.S. degree in communication engineering from the Harbin Institute of Technology, Weihai, China, in 2019. He is currently pursuing the M.S. degree in electronics and communication engineering with the Harbin Institute of Technology, Shenzhen, China. His research interests include hydroacoustic channel estimation and tracking, signal detection and estimation, and compression sensing.



RONGRONG GUO received the B.S. degree in electronic and information engineering from Jiangxi Science and Technology Normal University, Nanchang, China, in 2020. She is currently pursuing the M.S. degree in electronic and information engineering with the Harbin Institute of Technology, Shenzhen, China. Her current research interest includes underwater acoustic communication.

...